



## **Coarse to fine : toward an intelligent 3D acquisition system**

V Daval, Olivier Aubreton, Frédéric Truchetet

### **► To cite this version:**

V Daval, Olivier Aubreton, Frédéric Truchetet. Coarse to fine : toward an intelligent 3D acquisition system. Three-Dimensional Image Processing, Measurement (3DIPM), and Applications 2015, SPIE, Feb 2015, San Francisco, United States. <hal-01164146>

**HAL Id: hal-01164146**

**<https://hal.science/hal-01164146v1>**

Submitted on 16 Jun 2015

**HAL** is a multi-disciplinary open access archive for the deposit and dissemination of scientific research documents, whether they are published or not. The documents may come from teaching and research institutions in France or abroad, or from public or private research centers.

L'archive ouverte pluridisciplinaire **HAL**, est destinée au dépôt et à la diffusion de documents scientifiques de niveau recherche, publiés ou non, émanant des établissements d'enseignement et de recherche français ou étrangers, des laboratoires publics ou privés.



HAL Authorization

# Coarse to fine: toward an intelligent 3D acquisition system

V. Daval, O. Aubreton, F. Truchetet  
Le2i, UMR 6306 CNRS-Université de Bourgogne, France

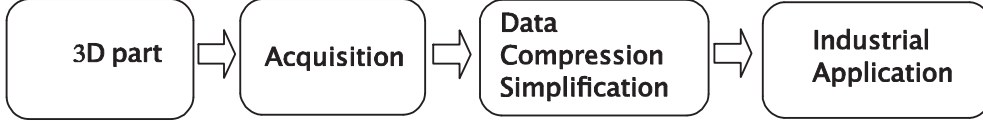
## ABSTRACT

The 3D acquisition-compression-processing chain is, most of the time, sequenced into independent stages. As resulting, a large amount of 3D points are acquired whatever the geometry of the object and the processing to be done in further steps. It appears, particularly in mechanical part 3D modeling and in CAD, that the acquisition of such an amount of data is not always mandatory. We propose a method aiming at minimizing the number of 3D points to be acquired with respect to the local geometry of the part and therefore to compress the cloud of points during the acquisition stage. The method we propose is based on a new coarse to fine approach in which from a coarse set of 2D points associated to the local normals the 3D object model is segmented into a combination of primitives. The obtained model is enriched where it is needed with new points and a new primitive extraction stage is performed in the refined regions. This is done until a given precision of the reconstructed object is attained. It is noticeable that contrary to other studies we do not work on a meshed model but directly on the data provided by the scanning device.

**Keywords:** 3D acquisition, normal estimate, 3D compression, 3D primitive extraction

## 1. INTRODUCTION

The 3D acquisition-compression-processing chain (see figure 1) is, most of the time, sequenced into independent stages.



As resulting, a large amount of 3D points (data) are acquired whatever the geometry of the object and the processing to be done in further steps. It appears, particularly in mechanical part 3D modeling and in CAD, that the acquisition of such an amount of data is not always mandatory. We propose a method aiming at minimizing the number of 3D points to be acquired with respect to the local geometry of the part and therefore to compress the cloud of points during the acquisition stage.

Very few approaches intending to process the data in the earliest stage of the acquisition chain can be found in the literature. Most of the works dealing with the use of local shape for compressing 3D data are based on mesh structured information. Amongst them the works of Yu et al. and of R. Bénére et al. can be quoted as being the most significative in the context of our approach<sup>1,2</sup>.

A larger state of the art presentation will include references to methods used at the different stages of our algorithm, including, as significative examples the works presented in<sup>3,4,5,6</sup> ...

## 2. METHOD

The method we propose is based on a new coarse to fine approach in which from a coarse set of 2D points associated to the local normals the 3D object model is segmented into a combination of primitives. The obtained model is enriched where it is needed and a new primitive extraction stage is performed in the refined regions. This is done until a given precision of the reconstructed object is attained. It is noticeable that contrary to<sup>2</sup> we do not work on a mesh but directly on the data provided by the scanning device.

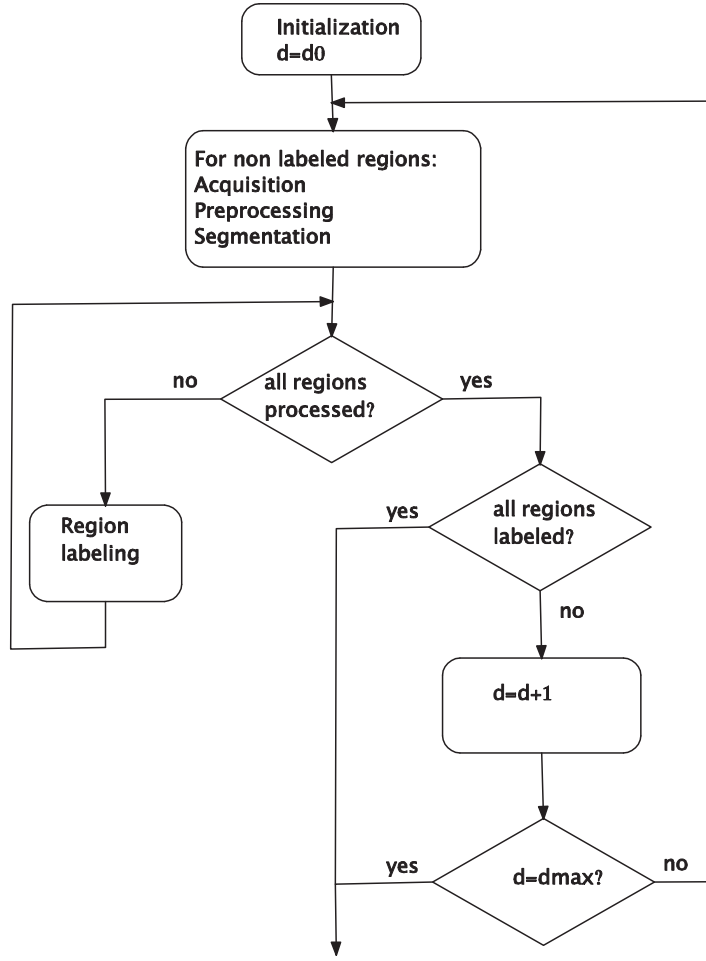


Figure 1. Global flowchart

The general coarse to fine algorithm is synthesized in the following diagram (figure 1).

We assume the 3D data are extracted at a given density  $d$  from 2D image(s) as in a large family of 3D scanning devices<sup>7</sup> as structured-light based sensing. Those set-up allows to extract the intensity of light coming from a given point as well as the normal vector associated (see figures 2 and 3).<sup>4</sup> The segmentation stage is region driven and it is based on a region growing algorithm using discontinuity measure as boundary criterion. For every region hence enclosed we try to identify a simple geometric primitive such as plane, cylinder, cone, sphere (or portion of). For doing that a PCA is done on the Gaussian sphere representation of the normals and a comparison with the surface rebuilt from the original 3D points is performed. If no such primitive can be found or if the reconstructing error is too large, another parametrized model is searched under the form of a Bézier surface. Once this done for all the regions, validated primitives are kept as well as the regions hence modelled. A more denser set of points is acquired for the remaining regions and the process is repeated. In the regions modeled by a Bézier surface, the process of refining is stopped when no change occurs for the associated model.

### 3. SEGMENTATION

The segmentation is done by region growing based on a feature extracted during the acquisition process: a local discontinuity measure. The local surface orientation, characterized by 3D normal orientation is also extracted

---

Frederic.truchetet@u-bourgogne.fr

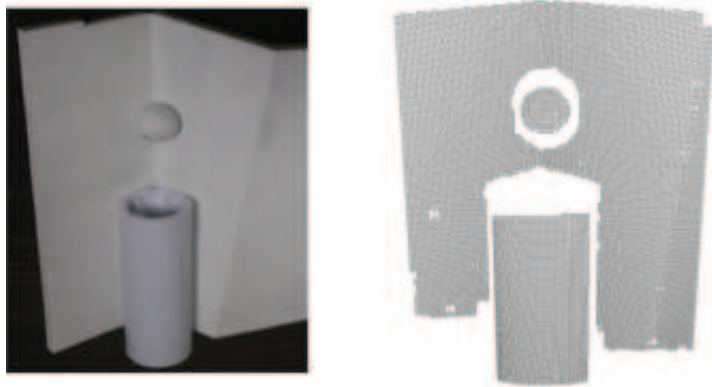


Figure 2. Example of data provided by the scanner: 2D image and 3D coordinates



Figure 3. 3D normals and estimated discontinuities

during the acquisition process for further primitive detection. Our acquisition set up is based on a lighting system projecting a pseudo random pattern on the object to be scanned; the stereo images are acquired by a calibrated set of two cameras.

### 3.1 Normal extraction

To extract normal from the pseudo random lighting pattern device we have adapted a method developed for structured lighting system by Song et al.<sup>8</sup> The principle of the method for structured lighting is based on a projected pattern which is a grid of points. The pattern used by the dense correlation method, meanwhile is a pseudo-random texture (Perlin noise<sup>9</sup>). However, with the latter method, one can match the points on a regular basis so as to reproduce a grid of points (called germs) and thereby apply the method<sup>10</sup> to Perlin noise as shown in Fig. 3. So we have re-implemented the method on a pseudo-random pattern and the results were compared between normals obtained by the structured lighting method and those given by dense correlation. In addition, we have also made a small change to the structured light approach, using four tangents instead of only two to improve the robustness of normal calculating. The figure 4 gives an illustration of the improvement brought by the 4-tangent method whatever the point density.

### 3.2 Local discontinuity or saliency estimate

As we aim at segmenting a 3D surface from a low density acquisition we need an estimate of the local curvature to detect boundaries on the scanned object. Unfortunately it is not easy to extract a local 3D curvature from the 2D images provided by our scanning set up. We propose a new discontinuity, or saliency, measure that can be estimated from the 2D image of the object enlightened by the random light pattern. We use the same grid of germs as the one used in the normal extraction. For a straight line  $i$  of such points seen in the first image

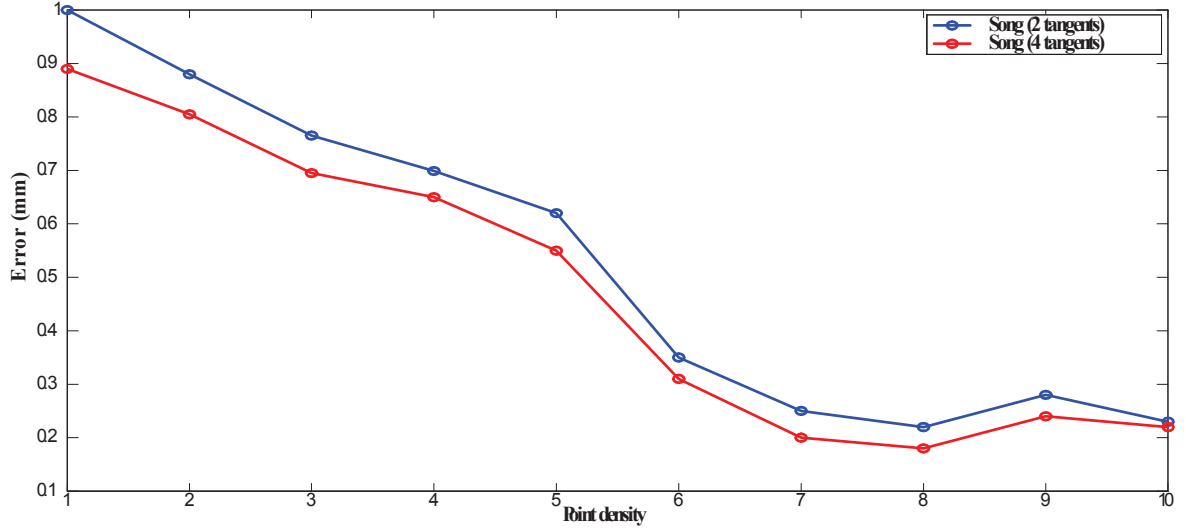


Figure 4. Comparison of the accuracy of the normal estimate for various point density with 2 or 4 tangents. The reference is computed on the highest density point cloud with a classical method.

(used as reference) the line drawn on the second image by the corresponding points is extracted and its local deformation is measured by the orientation of its 2D normal  $\mathbf{n}_{ji}$  on point  $P_j$  on the line (illustration in figure 5). The discontinuity coefficient is defined by

$$c_{ji} = \left| \frac{\mathbf{n}_{ji} \cdot \mathbf{n}_{j-1i} + \mathbf{n}_{ji} \cdot \mathbf{n}_{j+1i}}{2} \right|$$

with  $\mathbf{n} = (n_x, n_y)^t$

At every point  $j$ , 4 such discontinuity coefficients are measured along four different lines crossing at this point:  $i = 1, 2, 3, 4$  (1 : vertical, 2 : horizontal and 3, 4 : diagonals). The final saliency or discontinuity coefficient is the mean values of those four oriented coefficients.

$$C_j = \frac{\sum_{i=1}^4 c_{ji}}{4}$$

It must be noted that contrary to Dong et al.<sup>11</sup> the 3D cloud of points is not used for this measure rendering the method very efficient in term of computation weight. This saliency estimate can be performed whatever the point density and therefore it is well adapted to our approach. An example of normal and discontinuity measure is given in figure 3.

The data segmentation is done on the saliency image obtained from the previous stage. A region growing algorithm is used around a randomly chosen pixel. Once an homogeneous region is identified, it is labelled and removed from the image. The process is iterated up to the the last non labelled pixel.

#### 4. PRIMITIVE EXTRACTION

In every labelled region a gaussian sphere representation of the normals is used for the primitive identification stage. As we focus on 3D representations of mechanical parts and for simplicity reason we have chosen to consider only four simple kind of surface patches as primitives: plane, cylinder, cone and sphere. Each one can be described by a simple equation with very few parameters and it has a characteristic image on the gaussian sphere. The real data are more or less noised and the real surface geometry is never exactly one of the primitive

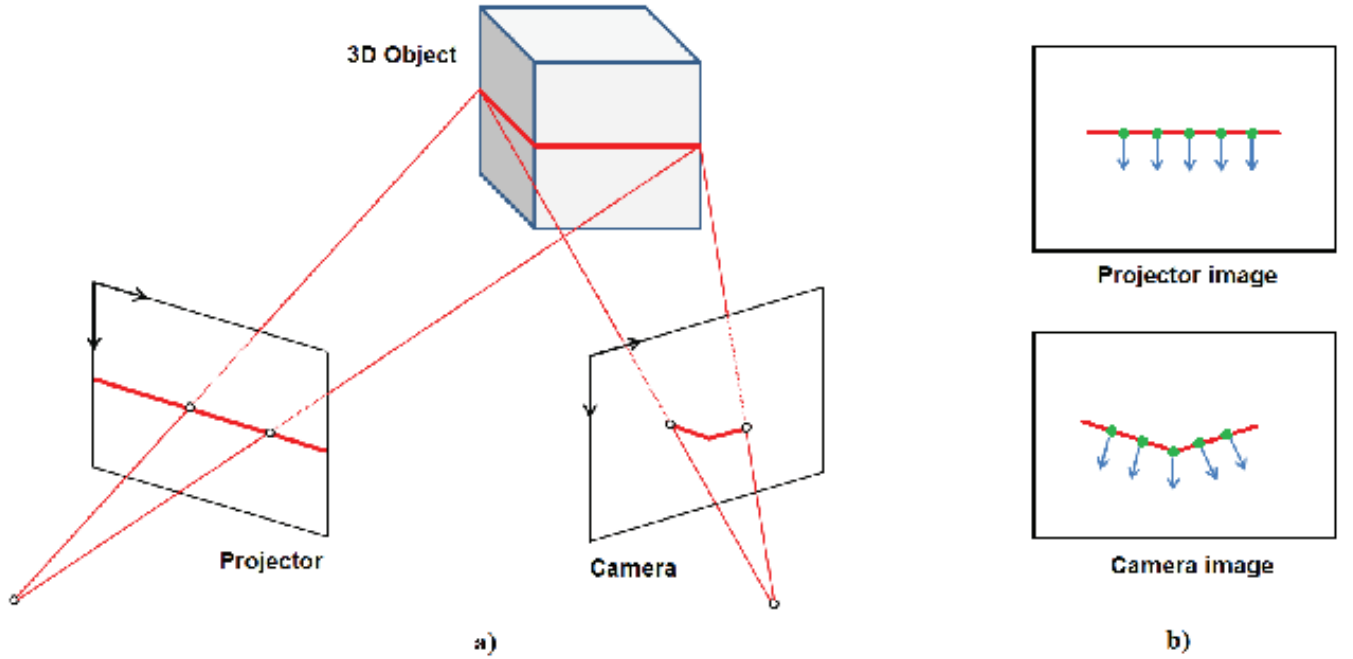


Figure 5. Principle of discontinuity estimate

set, hence to have a settable probabilistic approach of the identification we apply a PCA to the set of normals belonging to the given region and we proceed to the segmentation in the eigen value space. A learning stage using randomly (area, orientation, noise, curvature) built surface patches corresponding to the primitives allows to segment this feature space into 5 regions: no primitive, cone, cylinder, plane, sphere. Those regions are defined by rectangular boxes and the classification can be easily performed by simple thresholding of the eigen values. If a primitive is identified in a given region containing  $N$  points, the distance between the primitive and the 3D point cloud is computed, a given error threshold  $T$  and a ratio  $R$  of "good" points has been previously defined as global segmentation parameters. If the distance between points and surface is greater than  $T$  for more than  $R \cdot N$  points, the primitive is rejected. If the ratio  $R$  is not reached, the region is labelled with this primitive and no further increase of the local acquisition point density is needed. The points for which the error is greater than  $T$  are removed from the labelled set and they are considered as belonging to a non labelled region that must be refined in the next acquisition step. Even for industrial parts many regions cannot be identified to those very simple primitives and a more generic model must be used such as parametric local surfaces. We have chosen to fit Bézier surfaces rather than NURBS or B-spline.<sup>12</sup> Those surfaces have been designed by P. Bézier<sup>13</sup> to model car bodywork and they are well adapted to our problematic. They are built from Bernstein polynomials and, in our application, are locally designed following a 2D algorithm proposed by De Casteljaun.<sup>14</sup> An approximately regular quadrangular grid is set on the points belonging to non labelled regions and the best 3rd order Bézier patches are computed from the 3D points and their normals. The distance between the two Bézier patches obtained at two successive resolution (point density) is computed pointwise and if the mean distance is smaller than a given tolerance, we decide that the density from the previous step was high enough and the region will not be submitted to further refining by increasing the density of acquired points.

## 5. RESULTS

In the following figures an example of mechanical part acquisition is given.

In figure 6 an example of 2D image obtained with the coarsest density;  $d_0$  is set here so that 6991 points are acquired. At the end of the coarse to fine process, 5 primitives have been identified and 16323 points have been captured by the scanner. It must be denoted that with the finest density 41946 points should be acquired, a reduction of more than 60% is hence obtained.

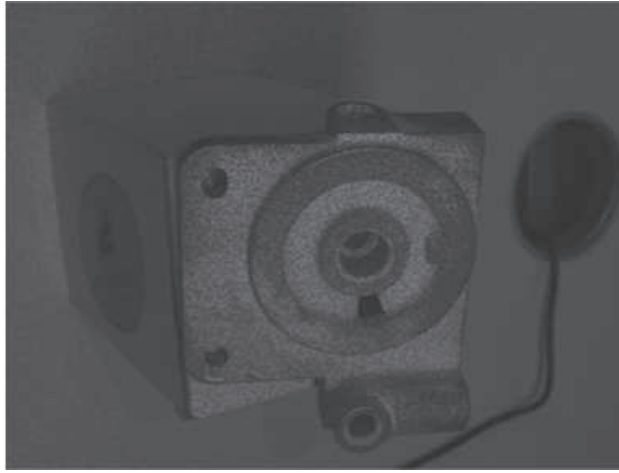


Figure 6. 2D image from the coarsest density acquisition

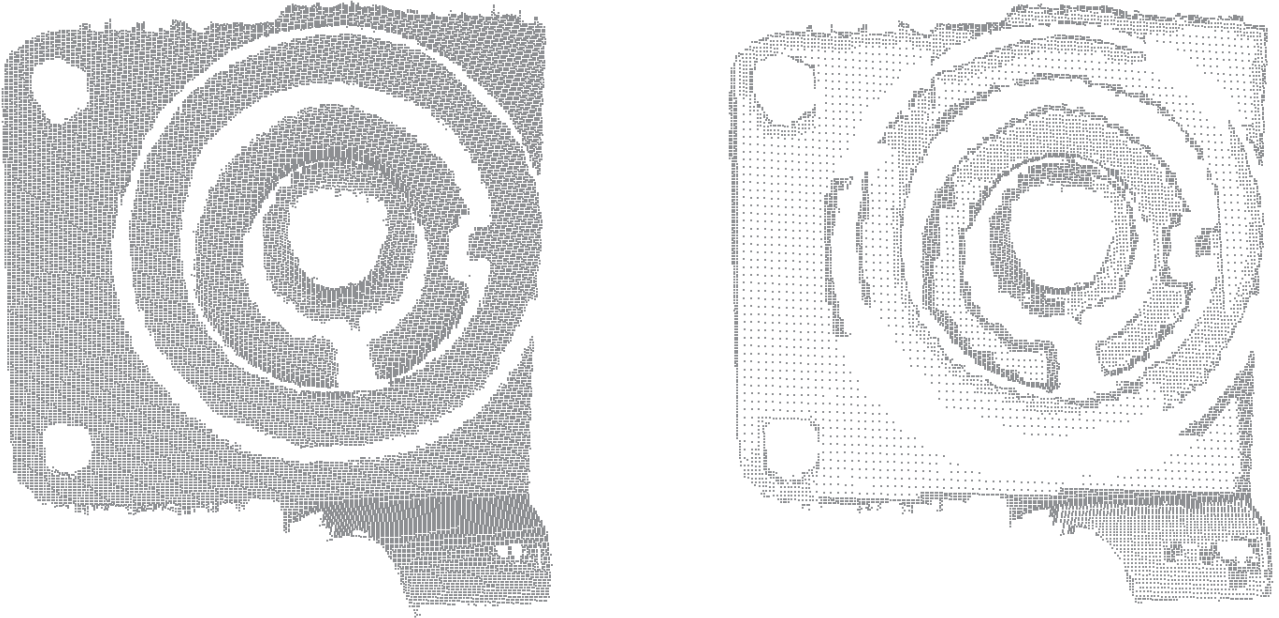


Figure 7. Two examples of point cloud; on the left, the finest density and on the right, the final necessary set.

An image of the cloud of points is given in figure 7. The maximum error, with respect to the finest possible resolution, has been set to 0.1 mm. To store the model, only about 12000 3D coordinates must be saved.

The curves in figures 11 and 12 illustrate the quality of the final cloud of point retained from our approach when we vary the tolerated threshold in the primitive identification stage. To evaluate our system we have tried to compare with existing methods. Unfortunately, as far as we know, no such approach has been used aiming at data simplification during the acquisition process. Generally 3D data simplification and compression are performed on meshes and not directly on the raw 3D point cloud. Two of the most reknown methods, whose software implementations are available are QSlim<sup>15</sup> and ACVD<sup>16</sup> methods. They propose edge preserving mesh simplification processes for which a compression ratio can be approximately specified and a final error can be computed. The comparison we have done for three different kind of industrial parts and for approximately the same simplification ratio shows the same final error is observed (figures 8, 9 and 10). This result illustrates how our approach allows to simplify the acquisition process and to lower the size of the 3D data file without significative loss on the reconstructed surface. Very few parameters must be set by the user:



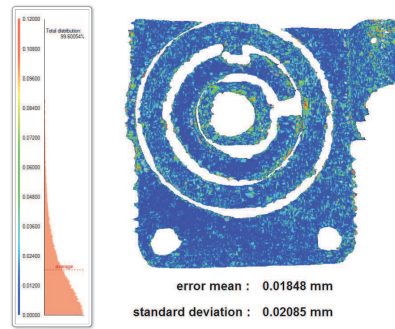


Figure 8. Example of ACVD, compression ratio : 51.32%

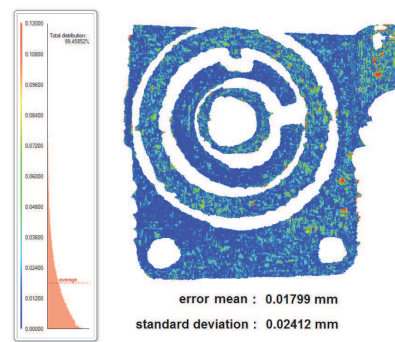


Figure 9. Our method, simplification ratio : 52.18%

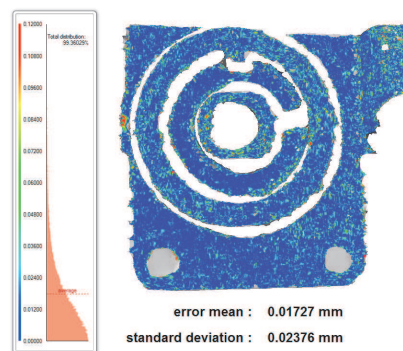


Figure 10. QSlim method, compression ratio : 51.03%



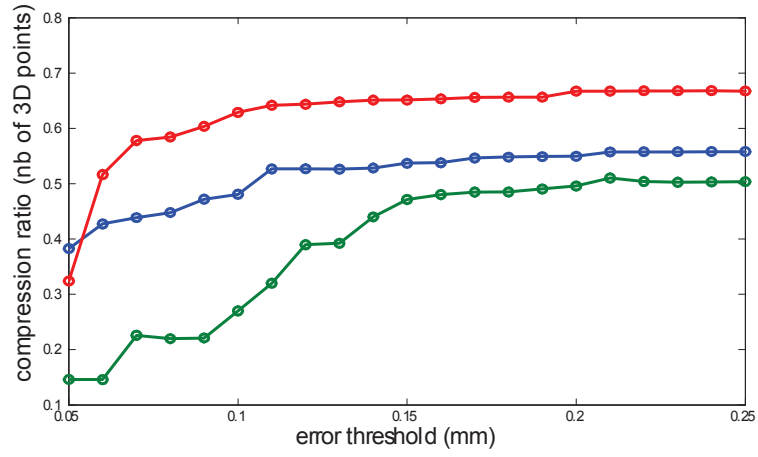


Figure 11. Simplification ratio with respect to error threshold for 3 different parts

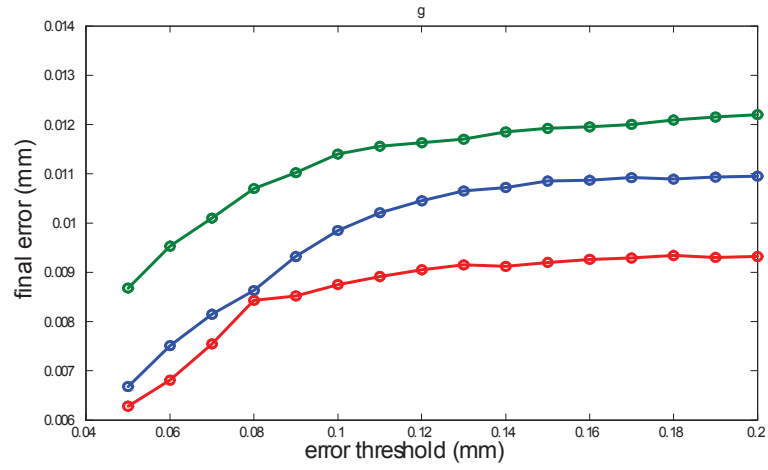


Figure 12. Final error (distance between the low density cloud retained from our approach and the highest possible density cloud of points) with respect to the tolerated error threshold.

- $T$ : maximum admitted reconstruction error
- $R$ : percentage of points used for a primitive identification within a region
- maximum and minimum density of points.

## 6. CONCLUSION

A complete "intelligent" 3D acquisition system is proposed in which only the necessary points are measured. This with respect to a given precision and, beside result, providing with a segmented model using, at least partially, high level geometric primitives. Those primitives can be used for point cloud compression, for a large sets of points can be replaced by the very few parameters of the primitives corresponding to the various identified patches.

Even if the approach can be generalized for any kind of shape by using more sophisticated primitives like parametric surfaces (nurbs, superquadrics or supershapes); with the simple high level primitives and the identification method used here, only mechanical parts can be efficiently considered.

## REFERENCES

1. L. Yu and X. Youlun, "Automatic segmentation of unorganized noisy point clouds based on the gaussian map," *Computer-Aided Design* **40**, pp. 576 – 594, 2008.
2. R. Bènière, G. Subsol, G. Gesquière, F. L. Breton, and W. Puech, "Recovering primitives in 3d cad meshes," in *proc. of Electronic Imaging*, SPIE, ed., january 2011.
3. H. Song and H. Feng, "A progressive point cloud simplification algorithm with preserved sharp edge data," *The International Journal of Advanced Manufacturing Technology* **45**, pp. 583–592, 2009.
4. Z. Song and C. Chung, "Determining both surface position and orientation in structured-light-based sensing," *Pattern Analysis and Machine Intelligence, IEEE Transactions on* **32**, pp. 1770–1780, 2010.
5. J. and P. Borrel, "Multi-resolution 3d approximations for rendering complex scenes," pp. 455–465, 1993.
6. D. Nehab and al., "Efficiently combining positions and normals for precise 3d geometry," *ACM Trans. Graphics* **24**(3), pp. 536–543, 2005.
7. V. Daval, F. Truchetet, and O. Aubreton, "Primitives extraction based on structured-light images," in *QCAV 13*, june 2013.
8. H. Song and H. Feng, "A progressive point cloud simplification algorithm with preserved sharp edge data," *The International Journal of Advanced Manufacturing Technology* **45**, pp. 583–592, 2009.
9. K. Perlin, "Improving noise," *ACM Trans. Graph.* **21**, pp. 681–682, 2002.
10. Z. Megyesi, G. Kos, and D. Chetverikov, "Dense 3d reconstruction from images by normal aided matching," *Machine Graphics and Vision* **15**, pp. 3–28, 2006.
11. C. Dong and G. Wang, "Curvatures estimation on triangular mesh," *Journal of Zhejiang Univ. SCI* **6A**, pp. 128–136, 2005.
12. R. H. Bartels, J. C. Beatty, and B. A. Barsky, *An Introduction to Splines for Use in Computer Graphics & Geometric Modeling*, Morgan Kaufmann Publishers Inc., 1987.
13. P. Bézier, "Courbes et surfaces," 1996.
14. W. Boehm and A. Muller, "On de casteljau's algorithm," *Computer Aided Geometric Design* **16**(7), pp. 587 – 605, 1999.
15. M. Garland and P. S. Heckbert, "Surface simplification using quadric error metrics," pp. 209–216, 1997.
16. S. Valette and R. Prost, "Wavelet-based multiresolution analysis of irregular surface meshes," *Visualization and Computer Graphics, IEEE Transactions on* **10**, pp. 113–122, 2004.